American Journal of Human Genetics, Volume *83*

Supplemental Data

Mutations in Glucose Transporter 9 Gene

SLC2A9 Cause Renal Hypouricemia

Hirotaka Matsuo, Toshinori Chiba, Shushi Nagamori, Akiyoshi Nakayama, Hideharu Domoto, Kanokporn Phetdee, Pattama Wiriyasermkul, Yuichi Kikuchi, Takashi Oda, Junichiro Nishiyama, Takahiro Nakamura, Yuji Morimoto, Keiko Kamakura, Yutaka Sakurai, Shigeaki Nonoyama, Yoshikatsu Kanai, and Nariyoshi Shinomiya

Table S1. Primer pairs used for sequence and restriction enzyme analysis of human *GLUT9* gene

Exon	Primer-forward	Primer-reverse	Amino acid changes	Restriction enzyme
Putative promoter isoform 1	5'-GAAGGGAAGACTGTTCTTGG-3'	5'-CTAGTATCAGAAGCCTGGAG-3'		
Putative promoter isoform 2	5'-GGGATGGAAGATTTTTGAGC-3'	5'-ACTCAGCCAACAGGAACTGAGTG-3'		
Exon 1a (5'UTR)	5'-TTCTTTGCTTGGCATTACCC-3'	5'-GCCTTGGCATTCAACATTC-3'		
Exon 2 (5'UTR + coding)	5'-GCAAACCTTTCGAAGACTGC-3'	5'-TTAACAGCCTCCCACTGACC-3'		
Exon 1b (5'UTR + coding)	5'-TCAAATTGCCACACTTCCTG-3'	5'-GCCTGCCTTCCCCACAG-3'		
Exon 3	5'-GGACAAAGACTTCTCCTCCG-3'	5'-CGCACCCGAAGGTTTCC-3'		
Exon 4	5'-TTGTTTTGTACACTGGCTTGC-3'	5'-GGACCCTGACAATGACACAG-3'		
Exon 5	5'-CTGGGATGGACAGTTCAGTG-3'	5'-CTCACATTTTGGGACACCC-3'		
Exon 6	5'-GTCCTCTGAAATGCACCTCC-3'	5'-GCACAGAAGATGCCTAAACAAACACA-3'	**R198C** (cgt→tgt)	***Alw*I**
Exon 7	5'-CAGTCCCCTCAACAATGACC-3'	5'-ATTGGCCCAGGTCCCAG-3'		
Exon 8	5'-CAGGGCCCAGCATTAGAC-3'	5'-CACCCTCTGATCCCTCCAG-3'		
Exon 9	5'-AGAAAATAGATTAAGTCCTTCCACTG-3'	5'-TGAACATTCCCACTGTGCTG-3'		
Exon 10	5'-GGTGACCATATCCATCCAG-3'	5'-GAAGGAGCACCTTAAGGTTG-3'	**R380W** (cgg→tgg)	***BtsC*I**
Exon 11	5'-ACCCATCAACCCATCATC-3'	5'-CCTTCTGTGGGATAGACTGC-3'		
Exon 12	5'-GTGTGGCAGATGGAGATGG-3'	5'-AGTGCTGCAGAATCAAAGGG-3'		
Exon 13-1 (coding)	5'-TTGAGCCAGCATCACACATGG-3'	5'-TCCTTGCAGCTTCCAGAAGGG-3'		
Exon 13-2 (3'UTR)	5'-TGCAGAAATCAGCCAGGCATT-3'	5'-GGTTGAGGGCAGGTCAAGGC-3'		

Primers for the analysis of *GLUT9* exon 10 were designed so that PCR amplification and the following *BtsC*I digestion result in one band (757 bp) from the normal controls, but an additional two bands (408 bp and 349 bp) from the R380W mutant samples. Primers for analysis of *GLUT9* exon 6 were designed based on a similar concept, so that PCR amplification followed by *Alw*I digestion results in two distinct bands (378 bp and 259 bp) from the normal controls, but in one band (637 bp) from the R198C mutant samples.

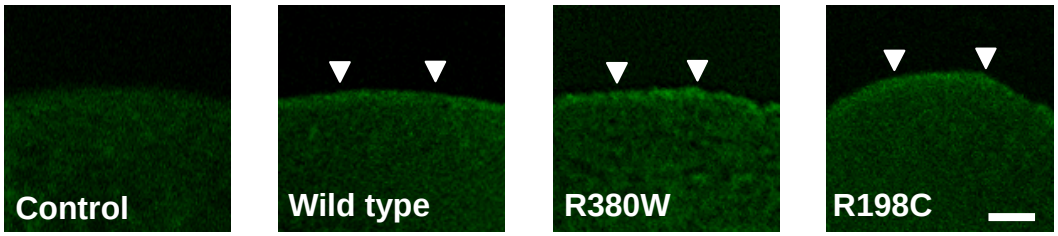

Figure S1. Subcellular localization of wild-type or mutated GLUT9 in oocytes.
Immunodetection with anti-GLUT9 shows that GLUT9L proteins (wild type, R380W, and R198C) are expressed on the plasma membrane (arrowheads), whereas fluorescence remains undetectable in water-injected control oocytes. Bar = 50 μm.

Species		R380W	R198C
Scientific name	Common name		
Homo sapiens	Human	F S G L V I E H L G **R** R P L L I G G F G L	Y L S E I S P K E I **R** G S L G Q V T A I F
Pan troglodytes	Chimpanzee	F S G L V I E H L G **R** R P L L I G G F G L	Y L S E I S P K E I **R** G S L G Q V T A I F
Macaca mulatta	Rhesus macaque	F S G L V I E H L G **R** R P L L I G D F G L	Y L S E I S P K K I **R** G S L G Q V T A I F
Monodelphis domestica	Gray short-tailed opossum	F S G L V I D R L G **R** R P L L I G G F G L	Y L S E I S P K E I **R** G S L G Q I T A I F
Mus musculus	House mouse	F S G L V I E R L G **R** R P L L I G G F G L	Y L N E I S P K E I **R** G S L G Q V T A I F
Echinops telfairi	Lesser hedgehog tenrec	F S G L V I E H L G **R** R P L L I G G F G L	Y L S E I S P K E I **R** G S L G Q V T A I F
Canis familiaris	Domestic dog	F S G L V I E R L G **R** R P L L I G G F G L	Y L N E I S P K E I **R** G A L G Q V T A I F
Ochotona princeps	American pika	F S G L A I E R L G **R** R P L L I G G F G L	Y L N E I S P K E L **R** G S L G Q V M A I F
Gallus gallus	Red junglefowl	S S G L V I E R L G **R** R P L L I G G F G L	Y L S E I S P K E I **R** G S L G Q V T A I F
Takifugu rubripes	Tiger puffer (Torafugu)	I S G L V I E R I G **R** K P L L I F G F T A	Y L G E I T P R H I **R** G S I G Q F N S I L
Gasterosteus aculeatus	Threespine stickleback	I S G L V I E R I G **R** K P L L I F G F S A	Y L G E I T P R H I **R** G S I G Q F N S I L
Oryzias latipes	Japanese medaka	I S G L V I E R I G **R** K P L L I F G F S S	Y L G E I S P R H I **R** G F I G Q F N S I L

Figure S2. Amino acid conservation in GLUT9 vertebrate orthologs.
Arginine residues orthologous to human GLUT9 amino acid positions 380 and 198, which are the sites of missense mutations identified in hypouricemia patients, are boxed in magenta.

Species	Transporter (amino acid)	Sugar transport proteins signature 1	Transporter (amino acid)	Sugar transport proteins signatures 2	Snonym
Homo sapiens	GLUT9 (371-387)	SGLVIEHLGRRPLLIG-G	GLUT9 (173-198)	IMGIDGGVALSVLPMYLSEISPKEIR	Glucose transporter 9 (SLC2A9)
	GLUT1 (324-340)	SLFVVERAGRRTLHLI-G	GLUT1 (128-153)	IIGVYCGLTTGFVPMYVGEVSPTALR	Glucose transporter 1 (SLC2A1)
	HMIT (362-378)	GVWLVEKVGRRKLTFG-S	HMIT (161-186)	VVGLGIGIASMTVPVYIAEVSPPNLR	Proton myo-inositol cotransporter (SLC2A13)
Saccharomyces cerevisiae	Hxt1 (377-394)	SLYTVDRFGRRNCLMWGA	Hxt1 (176-201)	ISGLGVGGITVLSPMLISEVAPSEMR	Low-affinity glucose transporter HXT1
	Hxt2 (368-385)	ALYTVDKFGRRKCLLGGS	Hxt2 (167-192)	ISGMGVGGIAVLSPTLISETAPKHIR	High-affinity glucose transporter HXT2
	Hxt3 (374-391)	SLYTVDRFGRRNCLLYGA	Hxt4 (182-207)	ISGLGVGGIAVLSPMLISEVSPKHIR	Low-affinity glucose transporter HXT3
	Hxt4 (383-400)	GIFLVERYGRRRCLLWGA	Hxt3 (173-198)	ISGLGVGGIAVLSPMLISEVAPKEMR	Low-affinity glucose transporter HXT4
	Hxt5 (398-414)	SLYTVDRFGRRNCLLW-G	Hxt5 (197-222)	ISGLGVGGITVLAPMLISEVSPKQLR	Probable glucose transporter HXT5
	Hxt6 (377-394)	GIYVVERYGRRTCLLWGA	Hxt6 (176-201)	ISGLGVGGIAVLSPMLISEVSPKHLR	High-affinity hexose transporter HXT6
	Hxt7 (377-394)	GIYVVERYGRRTCLLWGA	Hxt7 (176-201)	ISGLGVGGIAVLSPMLISEVSPKHLR	High-affinity hexose transporter HXT6
	Hxt8 (379-396)	SLYSVDKLGRRRCLLLGA	Hxt8 (178-203)	IAGIGAGSISVLAPMLISETAPKHIR	Hexose transporter HXT8
	Hxt9 (373-390)	AVYTIERFGRRTCLLWGA	Hxt9 (172-197)	ISGLGVGGIAVLSPMLISEVAPKQIR	Hexose transporter HXT9
	Hxt10 (361-378)	ALYIVDKFGRRKCLLWGS	Hxt10 (160-185)	VSGMGVGGVAVLSPTLISEISPKHLR	Hexose transporter HXT10
	Hxt11 (373-390)	AVYTIERFGRRTCLLWGA	Hxt11 (172-197)	ISGLGVGGIAVLSPMLISEVAPKHIR	Hexose transporter HXT11
	Hxt13 (370-387)	AVMVVDKIGRRKCLLFGA	Hxt13 (169-194)	IYGLGAGGCSVLCPMLLSEIAPTDLR	Hexose transporter HXT13
	Hxt15 (373-390)	AVMVVDKIGRRKCLLFGA	Hxt15 (172-197)	IYGLGAGGCSVLCPMLLSEIAPTDLR	Hexose transporter HXT15
	Hxt16 (373-390)	AVMVVDKIGRRKCLLFGA	Hxt16 (172-197)	IYGLGAGGCSVLCPMLLSEIAPTDLR	Hexose transporter HXT16
	Hxt17 (370-387)	AVMVVDKIGRRKCLLFGA	Hxt17 (169-194)	IYGLGAGGCSVLCPMLLSEIAPTDLR	Hexose transporter HXT17
	Itr1 (390-406)	AFFSIDKIGRRTILLI-G	Itr1 (188-213)	IMGFGVGIGSLIAPLFISEIAPKMIR	Myo-inositol transporter 1
	Pho84 (409-425)	SVFTVDIIGRKPIQLA-G	Pho84 (170-195)	VMGIGIGGDYPLSSIITSEFATTKWR	Inorganic phosphate transporter PHO84
	Ybr241C (349-366)	ASAIIDHVGRRPLLLAST	Ybr241C (147-172)	LVGMSCGTAIVITPLFINEIAPVEWR	Probable metabolite transport protein YBR241C
Escherichia coli	araE (314-330)	AVFTVDKAGRKPALKI-G	araE (121-146)	VLGIAVGIASYTAPLYLSEMASENVR	Arabinose-proton symporter
	galP (307-323)	AIGLVDRWGRKPTLTL-G	galP (114-139)	LLGLAVGVASYTAPLYLSEIAPEKIR	Galactose-proton symporter
	kgtP (299-316)	IGALSDKIGRRTSMLCFG	kgtP (133-158)	FQGLSVGGEYGTSATYMSEVAVEGRK	Alpha-ketoglutarate permease
	xylE (332-349)	AIMTVDKFGRKPLQIIGA	xylE (135-160)	IGGIGVGLASMLSPMYIAELAPAHIR	D-xylose-proton symporter
Arabidopsis thaliana	STP1 (338-355)	SIYGVDRWGRRFLFLEGG	STP1 (142-167)	LLGFGIGFANQAVPLYLSEMAPYKYR	Sugar transport protein 1
	INT2 (331-347)	SIYFIDRIGRKKLLII-S	INT2 (133-158)	LVGLGVGVASVTAPVYIAEASPSEVR	Probable inositol transporter 2
	SUGTL3 (312-329)	VMLTVDRWGRRPLLMISS	SUGTL3 (124-149)	FLGFGVGLISYVVPVYIAEITPKTFR	Sugar transporter ERD6-like 2
	PLST3 (346-362)	AVVLMDKLGRKVLLIG-S	PLST3 (155-180)	LVGIGMGIGPSVTALYVTEVSPAYVR	Probable plastidic glucose transporter 3

Pathogenic mutation sites for GLUT9 and GLUT1

Figure S3. Conserved arginine residues in sugar transport proteins signatures 1/2.
Pathogenic mutation sites (magenta) of GLUT9 (R380 and R198) and GLUT1 (R333 and R153) in consensus patterns 1/2 (blue) are highly conserved among the sugar transport proteins of yeast, bacteria, plants, and mammals. In the sugar transport proteins signatures 1 or 2, each residue (magenta) of the pathogenic mutation sites is found to be the most highly conserved arginine residue, which may be the determinant of membrane topology. Alignment data are retrieved from PROSITE (also see **Web Resources** and **Accession Numbers** in the main text), which shows perfect amino acid conservation in 374 or 350 sequences of transporters for sugar transport proteins signatures 1 and 2. Representative data of transport proteins from *Saccharomyces cerevisiae*, *Escherichia coli*, *Arabidopsis thaliana*, and *Homo sapiens* are shown in this figure.

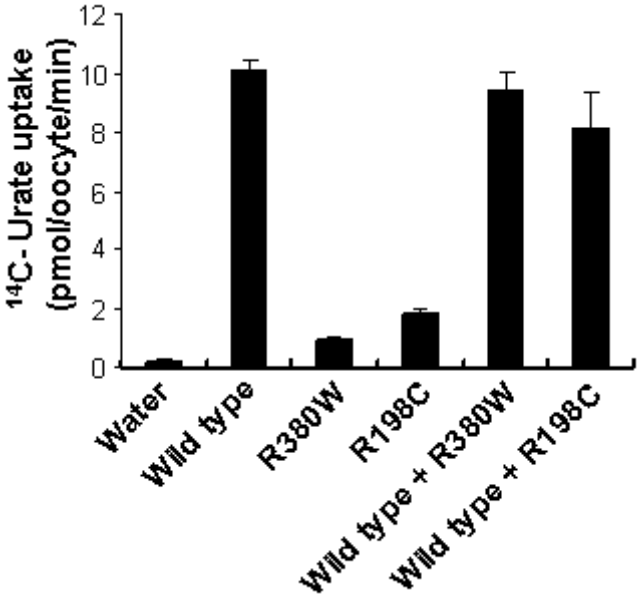

Figure S4. The effects of co-expression of wild-type and mutant GLUT9 on urate transport activities. Oocytes were injected with 12.5 ng of wild-type GLUT9L cRNA or mutant cRNA (R380W, R198C). For co-expression studies, both wild-type GLUT9L cRNA (12.5 ng) and mutant cRNA (12.5 ng) were co-injected to test the possibilities of dominant negative effects. Urate transport activities in oocytes injected with mutant cRNA (R380W, R198C) were markedly reduced, but those in co-injected oocytes (wild type + R380W, wild type + R198C) were not reduced. Results are expressed as mean ± SEM.

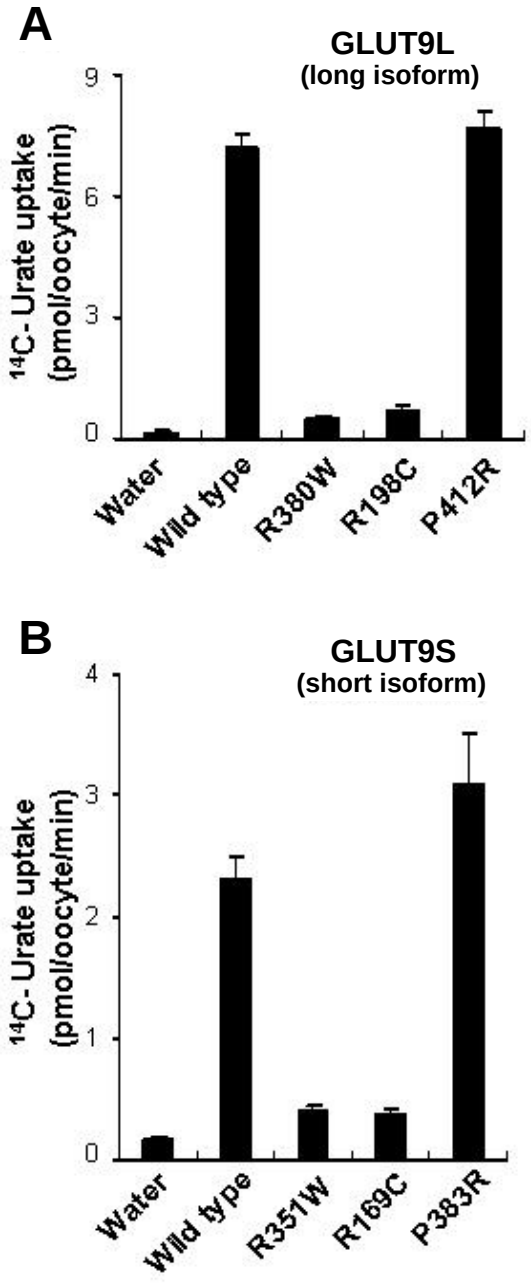

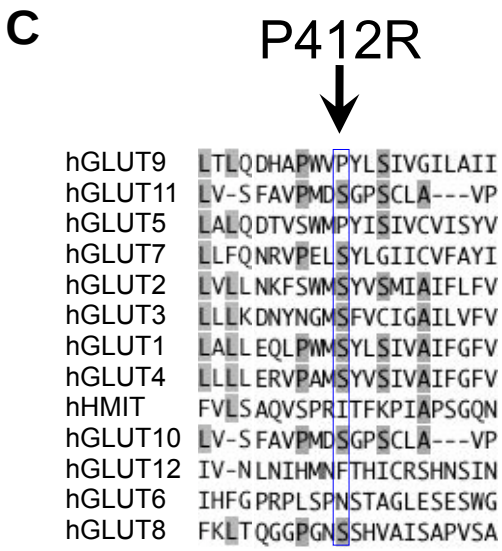

Figure S5. The P412R mutation is unlikely to be a pathogenic mutation for renal hypouricemia.
(A,B) The results of oocyte expression studies are displayed. Neither the P412R mutation in GLUT9L nor the P383R mutation in GLUT9S, which correspond to P412R in GLUT9L, reduced their urate transport activities at all. In contrast, pathogenic mutants of GLUT9L (R380W and R198C) and GLUT9S (R351W and R169C) markedly reduced their urate transport (4.6-10.8%). The extent of the reduction in urate transport from GLUT9 pathogenic mutations in our functional analyses are quite similar to those from URAT1 pathogenic mutations for renal hypouricemia. Also, the results from the GLUT9L mutants (A) are quite similar to those from the GLUT9S mutants (B), suggesting the reproducibility and reliability of the results. The reproducibility of the results was confirmed by three independent experiments using different batches of oocytes and *in vitro* transcribed cRNA. These data prove that P412R in GLUT9L and P383R in GLUT9S do not reduce the urate transport activities. Even if the P412R GLUT9 mutant showed moderate reduction in the urate transport activity as recently reported (about 60%) (Anzai, *et al*., J. Biol. Chem. 2008), the extent of functional reduction is not sufficient to cause clinical hypouricemia. These findings suggest that P412R is unlikely to be a pathogenic mutation for renal hypouricemia. Results are expressed as mean ± SEM. (C) The site of P412R is not conserved in the GLUT family transporters. In contrast, the pathogenic mutation sites R380W and R198C, which we identified in this study, are highly conserved in GLUT family transporters.

The extent of the reduction in urate transport (%) is calculated as follows; [(Uptake by mutant GLUT9-expressed oocytes) – (Uptake by control oocytes)] / [(Uptake by wild-type GLUT9-expressed oocytes) – (Uptake by control oocytes)] ×100.